This is an Accepted Manuscript, which has been through the Royal Society of Chemistry peer review process and has been accepted for publication.

Accepted Manuscripts are published online shortly after acceptance, before technical editing, formatting and proof reading. Using this free service, authors can make their results available to the community, in citable form, before we publish the edited article. We will replace this Accepted Manuscript with the edited and formatted Advance Article as soon as it is available.

You can find more information about Accepted Manuscripts in the Information for Authors.

Water Impact for Attached Paper:

Novel MOF Grown on Ni foam as a Ex Situ Absorptive Medium for the Remediation of
Hg Polluted Water in Surface Water

A novel metal-organic framework (MOF) coated on open-cell nickel foam was developed as a selective sorbent for Hg^{2+} in surface water, achieving high adsorption capacities at low concentrations. This paper demonstrates a new platform: MOF@foam, that can maximize the adsorptive capacities of MOFs compared to their powdered form. By exploiting this platform, and the benefits of hierarchical porosity that it confers, other MOFs may be developed to adsorb a large range of other persistent pollutants.

Novel MOF Grown on Ni foam as a Ex Situ Absorptive Medium for the Remediation of Hg Polluted Water in Surface Water

Authors:

E. Yosef[a], M. Halonur[a], D. Levy[a], and H. Mamane[a]

Affiliations:

a School of Mechanical Engineering, Faculty of Engineering, Tel Aviv University, Tel Aviv 69978, Israel

Author contributions:

Eitan Yosef executed the research and wrote the manuscript, Dr. Manohara Halonur assisted with fabrication, characterization, and kinetic analysis. Dr. Davide Levy performed the XRD analysis and provided and resolved a crystal structure therefrom. As principal investigator, Professor Hadas Mamane organized, directed, and provided executive advice and direction on the research.

Novel MOF Grown on Ni foam as a Ex Situ Absorptive Medium for the Remediation of Hg Polluted Water in Surface Water

1. Abstract

A novel metal organic framework (MOF) was fabricated on the surface of an open cell nickel foam and employed as a selective sorbent for Hg^{2+} dissolved in surface water. Two organic ligands (2-amino-teraphthalate and 4,4-dipyridyl) were combined with $Ni(NO_3)_2$ and grown on a Ni foam (95% porosity) to generate a P41 symmetric MOF with an internal 2.487 Å pore size and an active amino moiety serving as a binding site for Hg^{2+} and other heavy metals, characterized by XRD, and a lenticular crystal habit producing relatively well distributed spherical crystals, characterized by SEM-EDX. Adsorption experiments were conducted in both deionized water and mercury spiked into river water at concentrations typical for polluted areas ($[Hg^{2+}] \sim 4$, 40, and 400 ppb). The adsorption effect was characterized by Au-stabilized ICP-MS, finding highly favorable adsorptive efficacy, exhibiting adsorption capacities of 201.31 mg/g, 25.68 mg/g, and 3.017 mg/g, at initial concentrations of 400 ppb, 40 ppb, and 4 ppb, respectively. The coating of the MOF on the metal foam modulated the adsorption behavior of the MOF, maximizing the effective surface area of the adsorbent and thereby reversing the otherwise inverse relationship of % adsorbed with respect to increasing Ci.

2. Introduction

Mercury (Hg), like other heavy metal pollutants, has been studied extensively both as a highly dangerous and persistent pollutant and as a target for adsorption by functional absorptive materials [1]. The challenge of removing Hg from polluted water sources is particularly difficult, given its ability to produce ecocidal effects even at extremely low concentrations [2], the high concentration of other water constituents within polluted water, and the large volume of such water. Currently, there is no technology available that is efficient, selective, and cost-effective

enough to absorb and remove mercury from polluted water, which realistically present Hg concentrations in the low ppb range [3]. Metal Organic Frameworks (MOFs) have emerged as an attractive route to such a technology [4, 5, 6], with absorptive capacities (Qe) of some MOF materials reported as high as 0.0451 mg/g, even when the initial concentration (Ci) is as low at an initial concentration (Ci) of 12 ppb [7]. Other previously reported MOF materials are listed in Table 1, where Qe values are shown for the lowest Ci tested, given the proportional relationship between Ci and Qe.

Table 1: Comparison of Hg-Adsorbent MOFs in the Field

Material	Qe at min. Ci (mg/g)	Minimum Ci ([Hg]=ppb)	Time (minute)	Reference
BioMOF	2.05	10000	10080	8
Thiol-HKUST-1	0.008	8.1	1440	9
$Zn(hip)(L).(DMF)(H_2O)$	1.620	100	60	10
DUT-67	0.045	12	n/a	7
This work	0.003	4	60	

The internal porosity of MOF materials and the selective binding of moieties within the ligand structure, provide the basis for the highly effective absorption of particularly challenging pollutants like Hg. However, either the lack of any mesoporous or macroporous structural elements or the hydrophobicity of MOF surfaces, or more likely a combination of these factors, produce significant limits on Qe for powdered MOF materials. This problem is compounded in real surface water, rarely the subject of MOF absorption studies, where powdered MOF materials become fouled by otherwise common water constituents long before its ideal adsorptive capacity can even be reached.

Thus, a need exists to integrate MOF materials, and indeed other classes of adsorbents, with durable mesoporous or macroporous scaffolds to investigate the joint effect. Similar methods are already employed in the fabrication of permeable reactive barriers (PRBs), a class of technologies used for the *in situ* mitigation of damage to groundwater supplies from known contamination plumes underground [11]. PRBs are installed in the groundwater flow direction, and their permeability allows for water to pass through and dissolved contaminants to react with a PRB reactive surface. A similar method is also applied in the nano-selenium coating applied to the inner surface of a polyurethane foam, with exceptional results, albeit with expensive and fragile materials [12].

The same durability beneficial to metal foam materials' application as PRB could serve well as an application as a scaffolding for an *ex situ* reactive medium. Many types of foams are commercially available, and their surface chemistry can be easily modified by various methods for affixation of high performance sorbents for Hg. Much of the development of materials engineering of functional coatings on metal foams has been conducted in the electrochemical field, where various MOFs have been fabricated on metal foam materials for applications as electrical components [13,14]. The goal of the present study is to apply a MOF material grown selectively on the internal surface of a metal foam for the effective treatment of Hg contamination in realistic concentrations.

3. Materials and Methods

95% porosity open-cell Ni foam was sourced from Recemet, delivered from the Netherlands . 2-amino-teraphthalate, 4,4-dipyridyl, $Zn(NO_3)_2.6H_2O$ reagent grade 98, and dimethyl formamide (DMF) solvent were obtained from Sigma-Aldrich.

3.1. MOF@foam Synthesis

For each MOF@foam sample, 2-amino-teraphthalate (0.050 g), 4,4-dipyridyl (0.043 g), and $Zn(NO_3)_2.6H_2O$ (0.083 g) were mixed with 20 mL of DMF:ddH$_2$O (5:1) in a PTFE thermal reactor. Separately, circular pieces of Ni foam (diameter = 30 mm, height = 1.6 mm) with an

average weight of 0.486 g were sonicated for 10 minutes in 1 % HCl, then cleaned and sonicated with ddH$_2$O, until the cleaning solution registered a neutral pH. The foam was then added to the thermal reactor with the other reactants, and heated to 120 ^{o}C for 40 hours, then left to cool. The resultant MOF@foam composite was washed three times with 100 mL DMF, removing excess MOF material, then three times with 200 mL ddH$_2$O, then dried overnight at 60 ^{o}C, producing a MOF coating with an average mass of 39.5 mg over foams having an average 642 mg. The chemical formula of the resultant MOF coating was Zn(C$_{10}$H$_8$N$_2$)(C$_8$H$_5$NO$_4$).

3.2. Powder MOF Synthesis

An identical MOF was synthesized without the Ni foam substrate, wherein 2-amino-teraphthalate (0.05gm 2.8 mmol), 4,4-dipyridyl (0.043g, 2.8 mmol) and Zn(NO$_3$)$_2$.6H$_2$O (0.083g, 2.8 mmol as Zn) were mixed with 5 mL of DMF:ddH$_2$O (5:1) in a PTFE thermal reactor and heated to 120 ^{o}C for 40 hours, then left to cool. The resultant powder was washed with DMF, then ddH$_2$O, then dried overnight at 60 ^{o}C, producing a yellow MOF.

3.3. Absorption Experiments

Absorption of Hg was conducted in surface water collected from the Yarkon River in Tel Aviv and filtered with 0.45 µm membrane (from Millipore), then spiked with HgCl$_2$ to produce solutions of ~ [Hg]: 400; 40; and 4 ppb.. Other water quality parameters for the Yarkon River water were characterized by with a MRC-103 multiparameter probe, finding a conductivity of 1268 mS, a pH of 6.7, ORP of 183 mV, and calculating a hardness of 761 ppm equ. CaCO3. Absorption experiments were also conducted in Hg in ddH$_2$O for comparison, and further in ddH$_2$O containing similar concentrations of Hg, Cd, and Pb, to assess for selectivity. All [Hg] results were obtained with an Agilent 7500 ICP MS at Tel Aviv University, and all samples were made up to 2 % HCl and 5 % HNO$_3$ using ultrapure materials from Sigma Aldrich and were additionally stabilized with 1 ppm of Au from Sigma Aldrich Au ICP standard.

The Hg uptake, q_t (mg/g), which is the amount of adsorbed Hg at time t (min) on a specific amount of MOF@foam, was determined using the following equation:

$$q_t = \frac{(C_i - C_t) \cdot V}{m} \tag{1}$$

where C_i and C_t (mg/g) are the initial Hg concentration and the concentration at time t, respectively, V (L) is the volume of the solution, and m (g) is the dose of the adsorbent MOF material, which was derived from the mass difference between the composite and the raw unmodified foam. The percentage of Hg removal was calculated using the following equation:

$$\tag{2}$$

$$Hg\ Removal\ \% = \frac{C_i - C_t}{C_i} \cdot 100\%$$

Batch experiments were conducted in 50 mL volumes of Hg-containing solutions agitated at room temperature in a mechanical shaker incubator at 150 rpm. Sample volumes were passed through a 0.45 μm filter to remove any loose MOF particles, then diluted with a stabilization solution for ICP analysis.

Adsorption kinetics

Two linear forms of kinetic models were examined for the MOF@foam . The first model is the pseudo-first-order equation of Lagergren for the sorption of a liquid/solid system based on the solid capacity, which is the most widely used expression for liquid-phase sorption processes, and can be represented as follows:

$$\log(q_e - q_t) = -\frac{k_1 t}{2.303} + \log q_e \tag{1}$$

where q_e (mg/g) is the amount of Hg adsorbed per unit mass of MOF at equilibrium, and k_1 ($\min^{-1}$) is the rate constant of the pseudo-first-order model. This model can also be expressed as the differential equation (2) and then integrated into the linear equation (3).

$$\frac{\delta q_t}{\delta t} = k_t(q_e - q_t) \tag{2}$$

$$\frac{1}{k_1} \cdot \ln(q_e - q_t) = t$$

The second model is the Lagergren pseudo-second-order equation, expressed in the linear form (4):

$$\frac{t}{q_t} = \frac{t}{q_e} + \frac{1}{k_2 q_e{}^2} \qquad (4)$$

Where, k_2 $(g/mg \cdot min)$ represents the rate of the pseudo-second-order model.

3.4. Characterization

Scanning Electron Microscopy (SEM) was conducted with a Thermo Fisher Quanta 200 FEG ESEM instrument, which employs Energy-dispersive X-ray spectroscopy (EDS). Crystallinity was analyzed using powder x-ray diffraction (Empyrean II Diffractometer) operating with Cu–Kα1 radiation (I = 1.54 A˚) at a scan rate of 3° min-1 and a 2 theta range of 5-80°, using mercury software for analysis, and comparing to other known MOF crystal structures. Zeta potential was measured by an Anton Paar, SurPASS 3 instrument using 0.001M KCl, where streaming potential measurements were conducted at pH 7.

4. Results and Discussion

4.1. Materials Characterization:

SEM characterization demonstrates several features of the composite material and its fabrication method, including that the MOF coating is well distributed within the inner surface of the metal foam, as shown in Fig. 1a.

The foam is pre-treated with 1% HCl which likely activates the foam' surface for nucleation. Then, MOF is immobilized on the foam by selectively growing the MOF crystals on the internal surface of the Ni foam during the synthesis process. The forces keeping the MOF attached to the foam include chemical bonding between the MOF and the Ni foam surface, as well as physical adhesion due to rough surface itself. The MOF crystals preferentially crystallize on

the Ni foam's surface rather than forming free-floating particles, ensuring effective immobilization and the selective crystallization ensures a strong interaction between the MOF and the foam substrate.

Whilst the deposition of the MOF on the metal foam may not generate a nanometrially uniform layer throughout the complex internal geometry, the selectivity of MOF crystallization for the metal foam surface over existing MOF surfaces ensures the effective (exposed) surface area of the MOF material is significantly higher than for undeposited MOF material, raising its potential for adsorptive effects.

The MOF crystals themselves display, at the micrometric level, a lenticular crystal habit that generates sphere-like crystals each containing a high density of internal porosity, as shown in fig. 1b,. This microstructural porosity also provides ample opportunity for adsorbates in solution to penetrate within the MOF, further enhancing the potential for adsorption. The combination of macrometric, mesometric, micometric, and nanometric porosities, provides a hierachical porosity that allows the MOF material greater capitalization of its adsorption capacity.

EDS measurements coupled with the scanning electron micrographs indicate the stoichiometric ratio of elements contained within the MOF@foam composite surface correlates to the theoretical molecular structure of the MOF material.

Figure 1a: Scanning Electron Micrograph of MOF@foam Coating

Figure 1b: Scanning Electron Micrograph of MOF@foam Crystal Structure

Energy-dispersive X-ray spectroscopy results shown in table 2 indicate a close approximation of theoretical values for the composition of the MOF material. Depositing the MOF on a Ni foam produces some obscuring effects, most notably that the K-beta line of Ni (8.26 keV) is close to that K-alpha line of Zinc (8.64 keV), thus Zinc may be underdetected in the EDS. The underdetection of light elements such as N in low concentrations may explain why N is not detected in the EDS spectrum.

7

Table 2: Elemental Distribution Derived from EDS

Element	Wt %	Wt % Sigma	Atomic %	Theoretical Atomic % for MOF
C	41.44	0.69	63.05	69.12
O	22.80	0.50	26.05	20.48
Zn	7.18	0.39	2.01	10.4
Ni	28.57	0.50	8.89	*Not relevant*

Figure 2: XRD Spectrum of $P4_1$ MOF@Foam before (a) and after (b)

A resolution of the PXRD results of the MOF indicated a $P4_1$ structure, with a major peak at approximately 16°, indicative of a key crystalline facet in its tetragonal symmetry. Additional minor peaks at 5.5°, 11° (a double peak), 15°, 20°, 25°, and 26° suggest a complex lattice structure typical of MOF materials. The simulated PXRD pattern derived from the resolved CIF structure ($P4_1$ space group; a = 15.21 Å, c = 7.88 Å) aligns well with the experimental PXRD data. Notably, the intense peak 14.5° corresponds to the (0 1 0) reflection with a d-spacing of 7.88 Å, consistent with tetragonal symmetry and characteristic of MOFs adopting $P4_1$-type frameworks. As shwon in Figure 2, the PXRD spectra before and after Hg adsorption remain identical, indicating that the crystal structure of the MOF framework was retained. This stability suggests that Hg adsorption occurs through localized interactions – likely at the amino functional groups – without inducing significant structural rearrangement detectable by powder diffraction.

Figure 3: Resolved Crystal Structure and Pore Geometry of P41 MOF

Following resolution of the crystal structure form XRD data, P41 tetragonal geometry was identified, and the size of the pore in was calculated to be 2.487 Å, wherein both sides of the pore are adjacent to a nitrogen atoms in amide moieties able to coordinate and bind Hg^{2+}, among other divalent cations. The atomic sizes of Hg^{2+}, Hg^{1+}, and Hg^0, all of which exist as

stable species in surface water containing other salts and organic matter, are 1.10 Å, 1.25 Å and 1.55 Å, respectively, and thus the 2.487 Å is sufficient for Hg-binding. In fig. 3: dark grey represents carbon, light grey represents hydrogen; red represents oxygen; green represents nickel; and blue represents nitrogen.

4.2. Surface charge of MOF@foam

The addition of the MOF coating on the Ni foam produces a greater negative surface charge, attributable to the presence of the carboxylic acid groups of the coordinating groups in the 2-amino-teraphthalate ligands, which can be seen in figure 4. This extra negative surface charge, even on the mV scale, likely aids the adsorption of cations like Hg.

Figure 4: Zeta of MOF@foam vs foam

4.3. Adsorption of Hg by the MOF and MOF@foam composite:

Overviews of the adsorptions of Hg by the MOF@foam composites at three different concentrations (~4 ppb, ~40 ppb, ~400 ppb) were conducted in in triplicate, and analysed with respect to time, reaching a maximum q_t at 1 hour. The adsorption kinetics of the MOF@foam composite were found to adhere to a pseudo 2nd order kinetic model, with the exception of initial period of adsorption at the lowest range tested ([Hg] ~4 ppb), see table 3 and figure 6a, the latter of which adheres to a pseudo 1st kinetic model. This indicates that at lower concentrations the physi-sorptive effect is more pronounced than the chemi-sorptive effect, which is consistent with both the highly nano, micro, and microporous structure of the MOF@foam composite and the relatively low affinity of the amide group for Hg, when compared to thiol groups or precious metal nanoparticles. Analysis for Zn was also undertaken to determine leaching into the samples from the MOF coating, finding negligible change in concentration, indicating that loose MOF coating was removed during the washing step of the fabrication.

Table 3: Kinetic Models of Hg Batch Adsorption

Parameter		[Hg] ~ 4 ppb	[Hg] ~ 40 ppb	[Hg] ~ 400 ppb
$q_e^{experimental}$ (µg/g)		3.017	25.68	201.31
Pseudo 1st Order	$q_e^{calculated}$ (µg/g)	2.289	20.81	186.42
	Δq (%)	24.1 %	19 %	7.4 %
	R^2	0.905	0.883	0.891
	k_1 (min^{-1})	0.126	0.0408	0.166
Pseudo 2nd Order	$q_e^{calculated}$ (µg/g)	3.215	28.21	215.67
	Δq (%)	6.56 %	9.86 %	7.13 %
	R^2	0.929	0.994	0.996
	k_2 (min^{-1})	0.00331	0.00221	0.000223

The initial adsorption (up to t = 45 minutes) in filtered freshwater fits very closely to the pseudo first order kinetic model, demonstrating an R-value much higher than that for all data points, indicating a lack of competition of Hg^{2+} for amide active sites in the MOF@foam, crucial for practical application. After this initial period the adsorption relationship becomes more chemi-sorptive in character, due to competition for the active sites, a relationship maintained at higher concentrations, see figures 6b and 6c. The initial period of adsorption with Hg ~ 40 ppb, as shown in Figure 5b, also indicates non-pseudo 2nd order kinetics, albeit for an initial few minutes.

Due to the proportional relationship between C_i and q_t values, q_t (and q_e) values for many adsorbents at the low concentrations realistically found in contaminated surface water are in the µg/g range [3]. This work found that at [Hg] ~ 4 ppb, the range of likely sorption capacities is between 200 and 350 µg/g, with equilibrium typically reached within 1 hour, as shown in Fig. 5a. For higher initial concentrations of 40 ppb and 400 ppb, the adsorption capacities were found in a range of 1.6 to 2.6 mg/g and 32 mg/g to 38 mg/g, as shown in fig. 5b and 5c, respectively.

The very high q_t values – given the initial concentrations – displayed by the MOF coating on the metal foam are facilitated by the maximization of exposure of the MOF to the influent fluid and minimizing the mass of MOF actually used for adsorption.

Figure 5: Adsorption Kinetics for MOF@foam in Freshwater

Adsorption by MOF@foam of [Hg]: (a) pseudo-1st order when [Hg] ~ 4 pbb in Filtered Freshwater; (b) pseudo-2nd order when [Hg]~ 40 ppb in Filtered Freshwater; (c) pseudo-2nd order when [Hg]~ 400 ppb in Filtered Freshwater

The deposition of the MOF material on the internal surface of the Ni foam modulates the relationship between the MOF's adsorptive effect and the initial concentration, to produce a logarithmic correlation indicating that the effective surface area of non-deposited MOF material represents a limitation to % Hg removal that is effectively overcome by deposition on the surface. Lower % Hg removals at lower initial concentrations for the MOF@foam composite in figure 6 are likely due to the batch adsorption nature of the experiment: without a means of forcing the solution through the internal geometry of the composite, flow effects produce a limiting factor on the extent of penetration and thus of adsorption.

Maintaining the metal foam material – which constitutes the most cost-prohibitive aspect of the MOF@foam composite – is paramount for sustainability, and thus the used composite material was stripped under 5% HCl and sonication for 60 minutes, then redeposited with the MOF material using the same hydrothermal deposition procedure described in the Materials and Methods section. The resultant MOF coating can then be used for Hg batch adsorption, the results of which are shown in figure 7. In order to account for the differences in Ci in the experimental procedure, figure 7 is shown with partition coefficient, which is equivalent to (Qe / Ce) ·V$_{exp}$, which provides a measure of the adsorptive effect independent of initial concentration, allowing for comparisons. As can be seen, with the exception of the higher concentration, the MOF@foam material demonstrated broadly consistent adsorptive effects through multiple cycles, indicating that neither the deposition or removal process affects the

surface of the metal foam in a way that compromises the adsorptive relationship between the MOF and the Hg, as seen in figure 7.

Figure 6: % Removed of MOF@foam vs Naked MOF at Different C_i

The kinetics of adsorption for Hg by the MOF@foam varies consistently with initial concentration, demonstrating a closer fit to a pseudo first order kinetic model at lower concentrations and a closer fit to a pseudo second order kinetic model at higher concentrations. This indicates that at lower concentrations the physi-sorptive effect is more pronounced than the chemi-sorptive effect, which is consistent with both the highly nano, micro, and microporous structure of the MOF@foam composite and the relatively low affinity of the amide group for Hg, when compared to thiol groups or precious metal nanoparticles.

Figure 7: Cycle Efficiency for Hg Removal **Figure 8:** Adsorption of Other Heavy Metal Ions

Batch adsorption was also carried out with ddH_2O in which both Cd and Pb were also dissolved, all at 100 ppb, at three pH levels (5, 7, and 9), finding slight favorability for Hg over Cd and Pb, as shown in figure 8. The MOF coating shows increasing adsorption of Hg as pH decreases, owing to the enhanced protonation of amino functional groups at lower pH, facilitating electrostatic attraction of Hg species. The adsorption of Cd shows the opposite behavior due to the increased formation and availability of negatively charged Cd hydroxide complexes at higher pH, enhancing electrostatic interactions. Adsorption of Pb by the MOF reaches a minimum at neutral pH and significantly higher levels at both acidic and basic conditions, likely due to competitive formation of different Pb species at varying pH conditions, promoting adsorption through either electrostatic attraction at acidic pH or precipitation and surface complexation at basic pH.

5. Conclusion

Coating the MOF material on the internal surface of the foam produced a durable MOF@foam composite with enhanced adsorption characteristics, maintaining pseudo 1st order kinetics at very low concentrations (<40 ppb) and pseudo 2nd order kinetics at higher concentrations still within the ppb range. In this study, Hg is an example of possible adsorbate present in low concentrations in high matrix water, such as the freshwater, wherein the designed P41 dual-ligand Zn-MOF's adsorption was improved by coating on a foam. This MOF@foam platform can therefore be applied to a number of other MOF systems, by appropriately activating the surface of the foam to form a nucleating surface, and lowering the concentration of reactants in the synthesis to produce preferential crystallization thereon. Utilization of such a MOF@foam platform should investigate the electro-sorptive applications, wherein the metal foam conductivity is leveraged to enhance selectivity and kinetics with fine control of the surface voltage.

References

1. J.G. Yu, B.Y. Yue, X.W. Wu, et al., Environmental Science and Pollution Research 23 (2016) 5056–5076. https://doi.org/10.1007/s11356-015-5782-7.

2. D.W. Boening, Chemosphere 40 (2000) 1335–1351. https://doi.org/10.1016/S0045-6535(99)00346-4.

3. V. Kumar, A. Sharma, R. Kumar, R. Bhardwaj, A.K. Thukral, J. Rodrigo-Comino, Human and Ecological Risk Assessment: An International Journal 26 (2020) 1–16. https://doi.org/10.1080/10807039.2018.1553610.

4. P.A. Kobielska, Coordination Chemistry Reviews 358 (2018) 92–107. https://doi.org/10.1016/j.ccr.2017.12.001.

5. G.R. Xu, Z.H. An, K. Xu, Q. Liu, R. Das, H.L. Zhao, Coordination Chemistry Reviews 427 (2021) 213554. https://doi.org/10.1016/j.ccr.2020.213554.

6. F. Zadehahmadi, N. T. Eden, H. Mahdavi, K. Konstas, J. I. Mardel, M. Shaibani, P.C. Banerjee, and M. R. Hill, (2023) Environmental Science, Water Research and Technology, 9, 1305

7. S. Chen, F. Feng, S. Li, X.-X. Li, L. Shu, Chemical Speciation & Bioavailability 30 (2018) 106–99. https://doi.org/10.1080/09542299.2018.1463832.

8. M. Mon, F. Lloret, J. Ferrando-Soria, C. Martí-Gastaldo, D. Armentano, E. Pardo, Angewandte Chemie International Edition 55 (2016) 11167–11172. https://doi.org/10.1002/anie.201606572.

9. K. Fei, et al., Journal of Hazardous Materials 196 (2011) 36–43. https://doi.org/10.1016/j.jhazmat.2011.08.087.

10. J. Zhou, H. Zhang, T. Xie, Y. Liu, Q. Shen, J. Yang, L. Cao, J. Yang, Journal of Environmental Science 119 (2022) 33–43. https://doi.org/10.1016/j.jes.2021.06.004.

11. J. Song, G. Huang, D. Han, Q. Hou, L. Gan, M. Zhang, Journal of Cleaner Production 319 (2021) 128644. https://doi.org/10.1016/j.jclepro.2021.128644.

12. S. Ahmed, J. Brockgreitens, K. Xu, A. Abbas, Advanced Functional Materials 27 (2017) 1606572. https://doi.org/10.1002/adfm.201606572.

13. K. Huang, S. Guo, R. Wang, S. Lin, N. Hussain, H. Wei, B. Deng, Y. Long, M. Lei, H. Tang, H. Wu, Chinese Journal of Catalysis 41 (2020) 1754–1760. https://doi.org/10.1016/S1872-2067(20)63510-4.

14. G. Zhi, X. Qi, Y. Li, J. Wang, J. Wang, Separation and Purification Technology 328 (2024) 124927. https://doi.org/10.1016/j.seppur.2023.124927
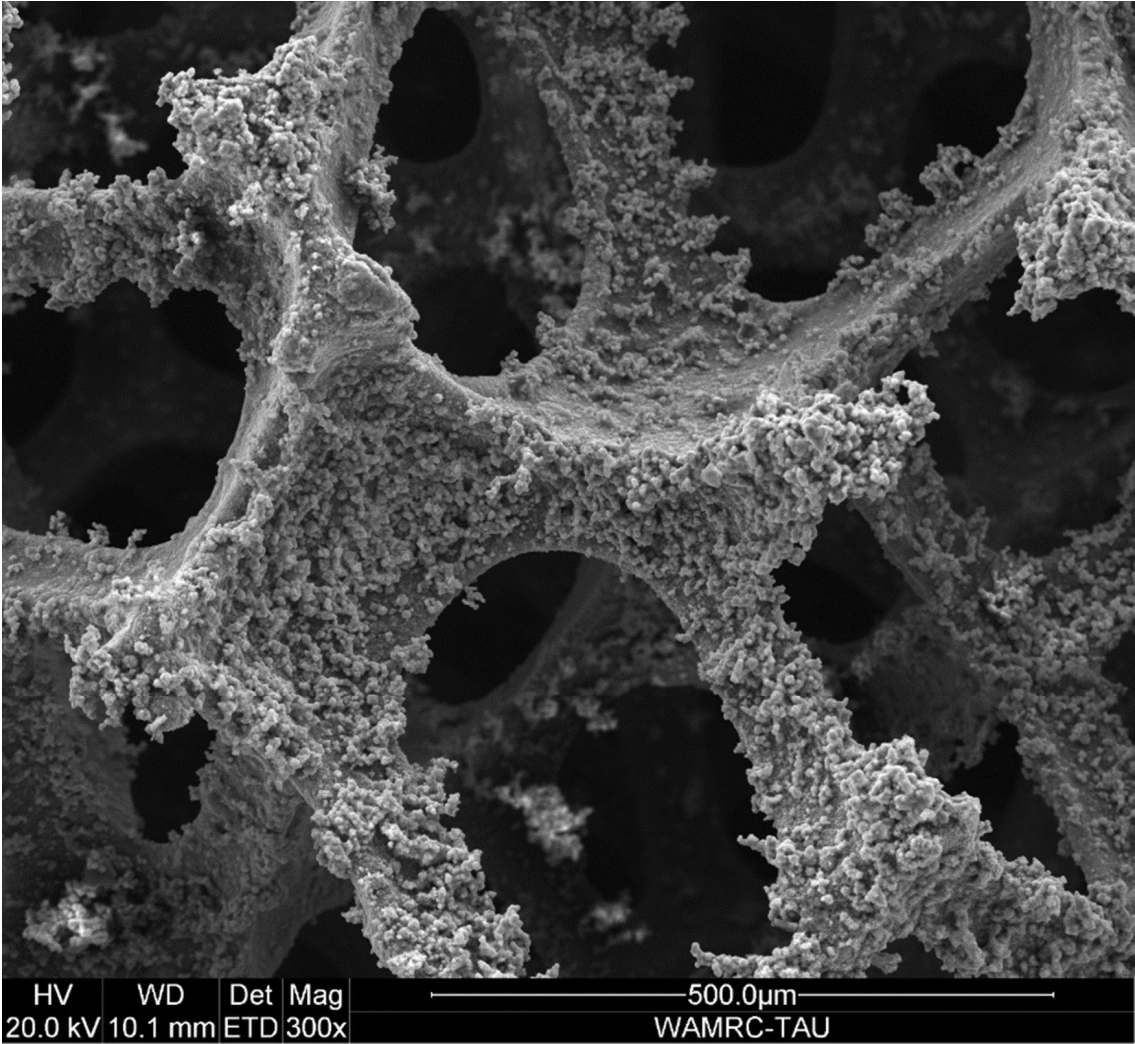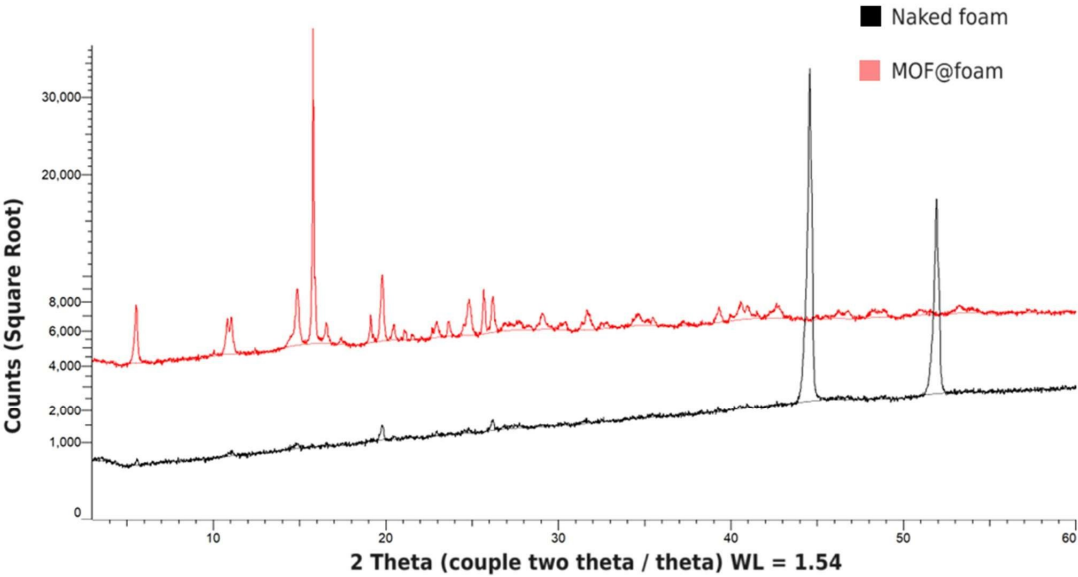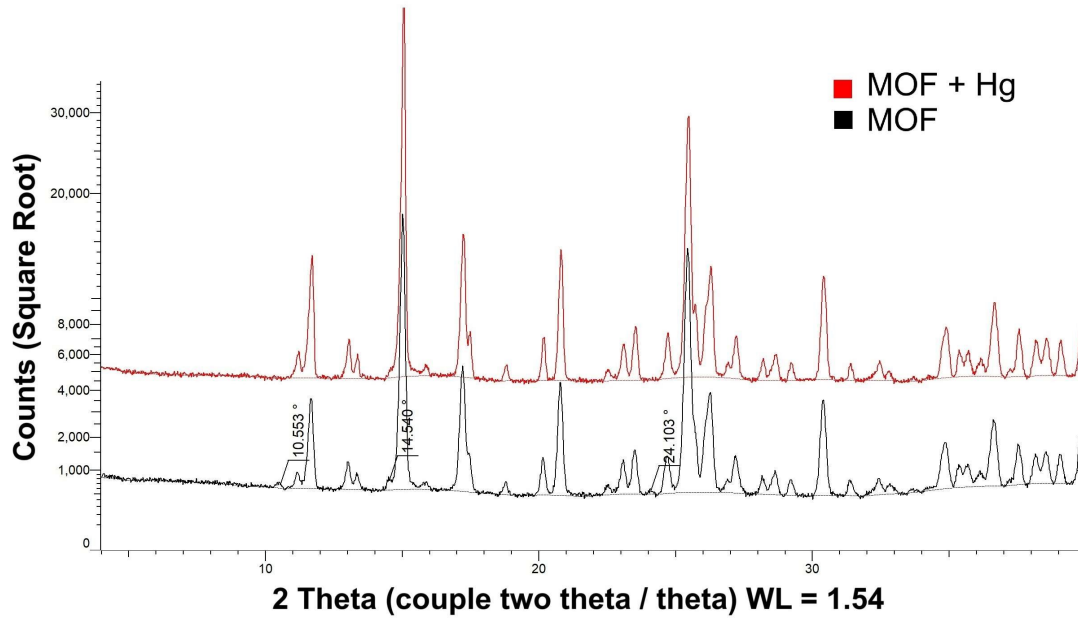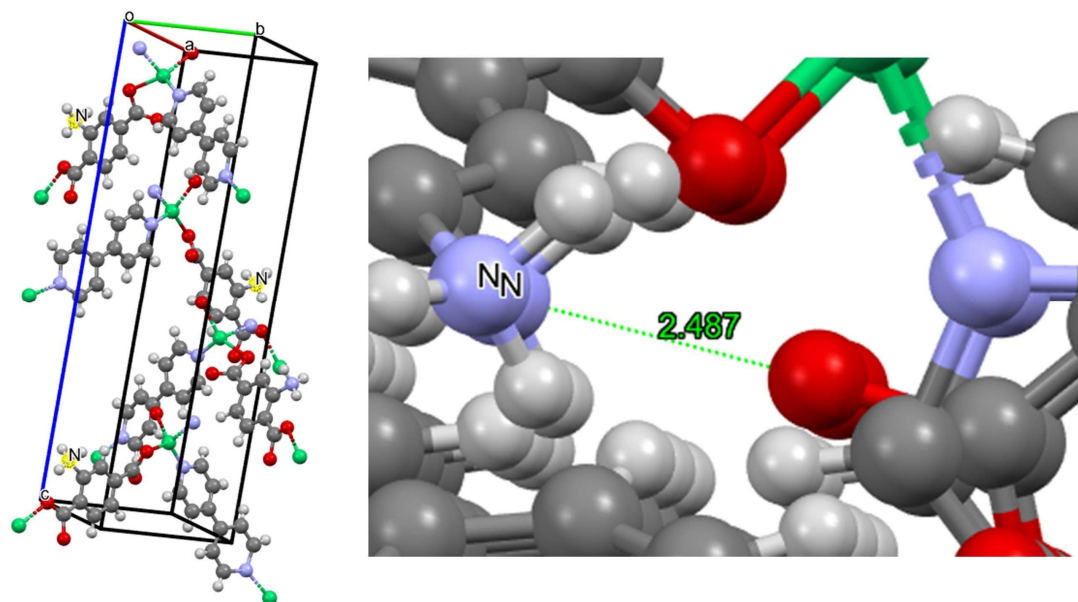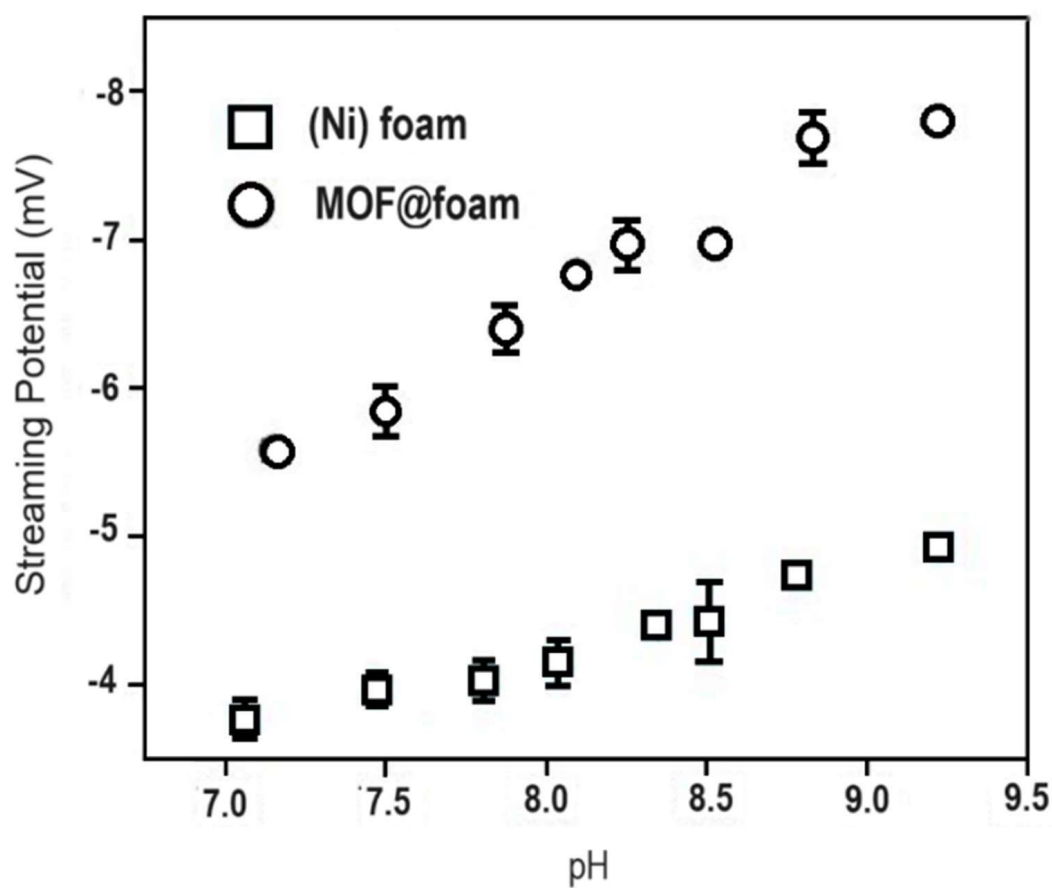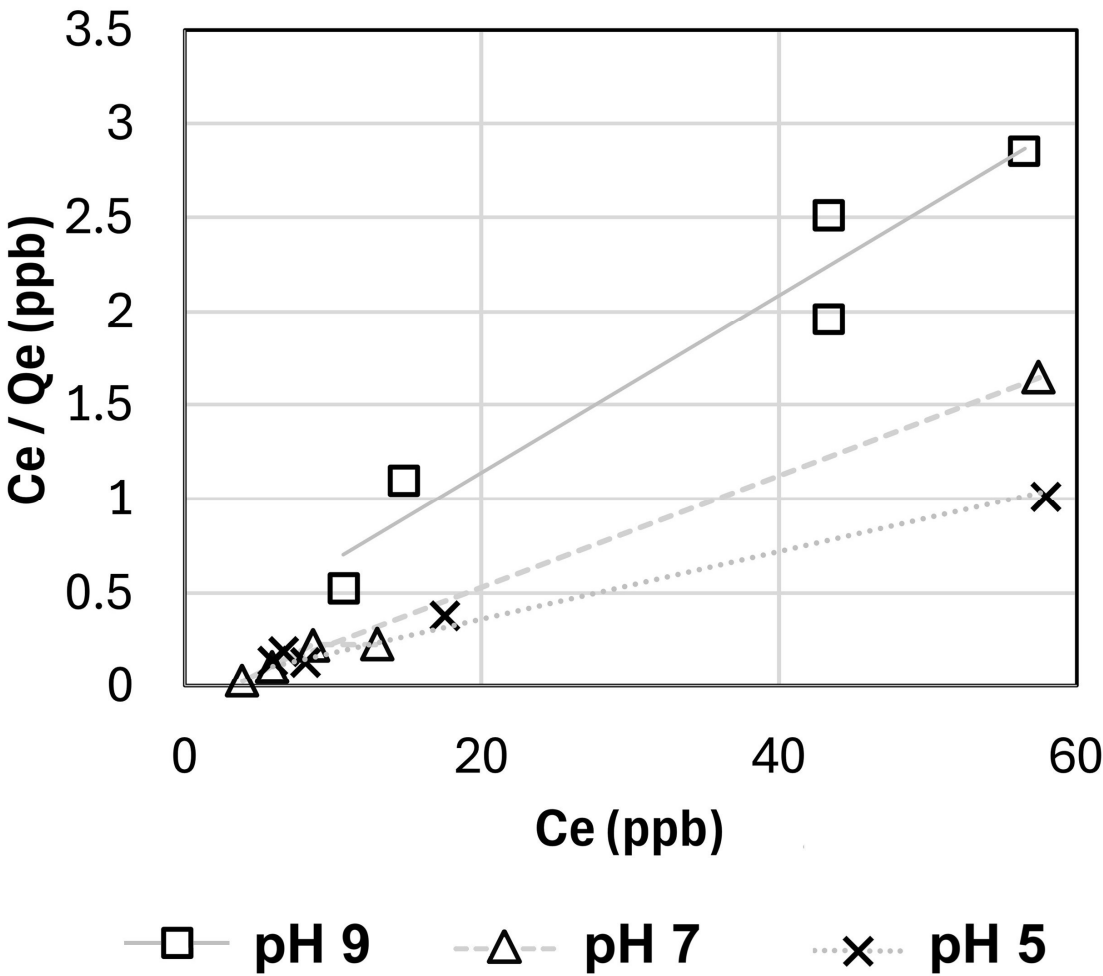
Figure 1A

Figure 1B
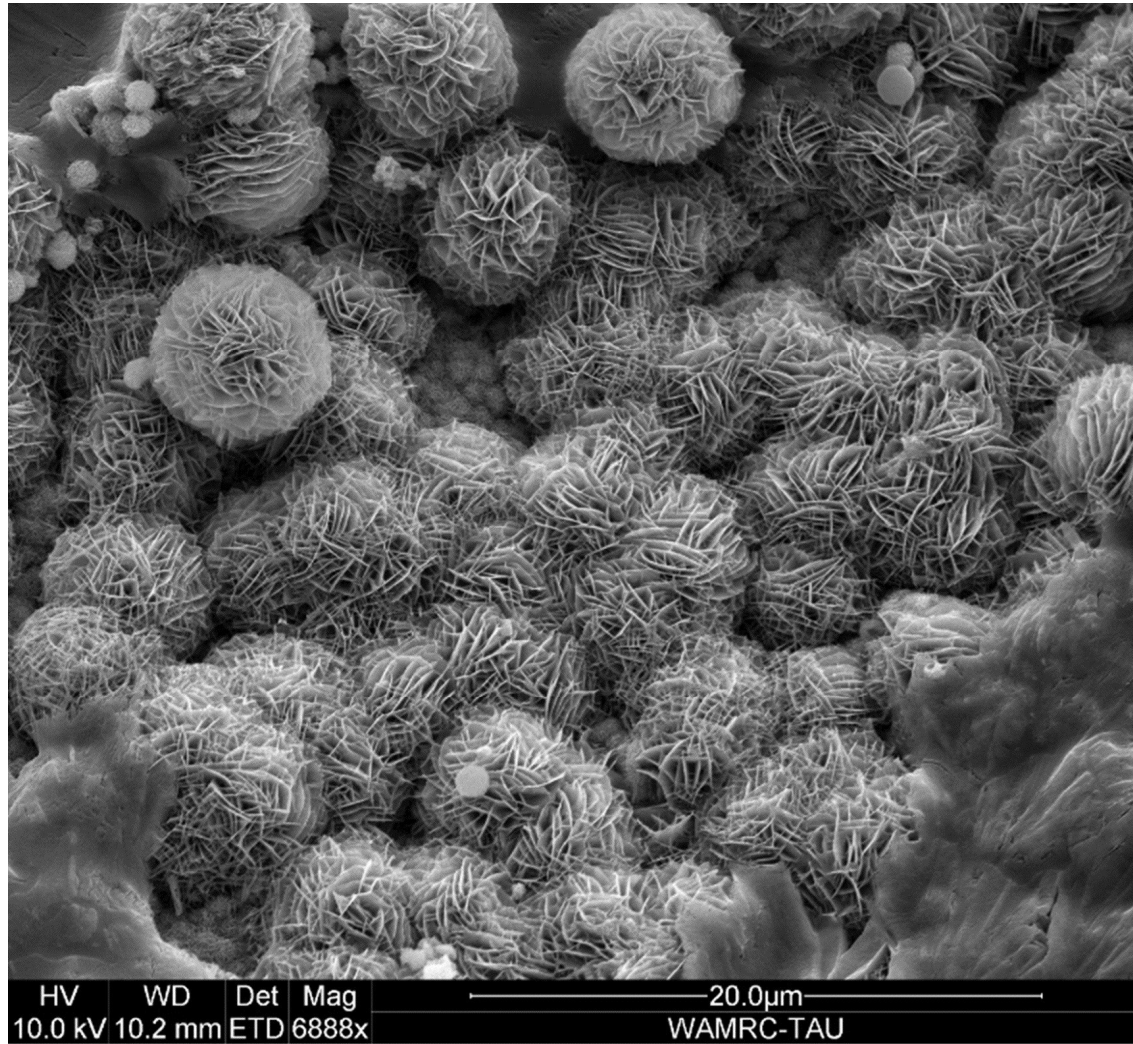
Figure 2A

Figure 2B

Figure 3

Figure 4

Figure 5

Figure 6

Figure 7

Environmental Science: Water Research & Technology Accepted Manuscript
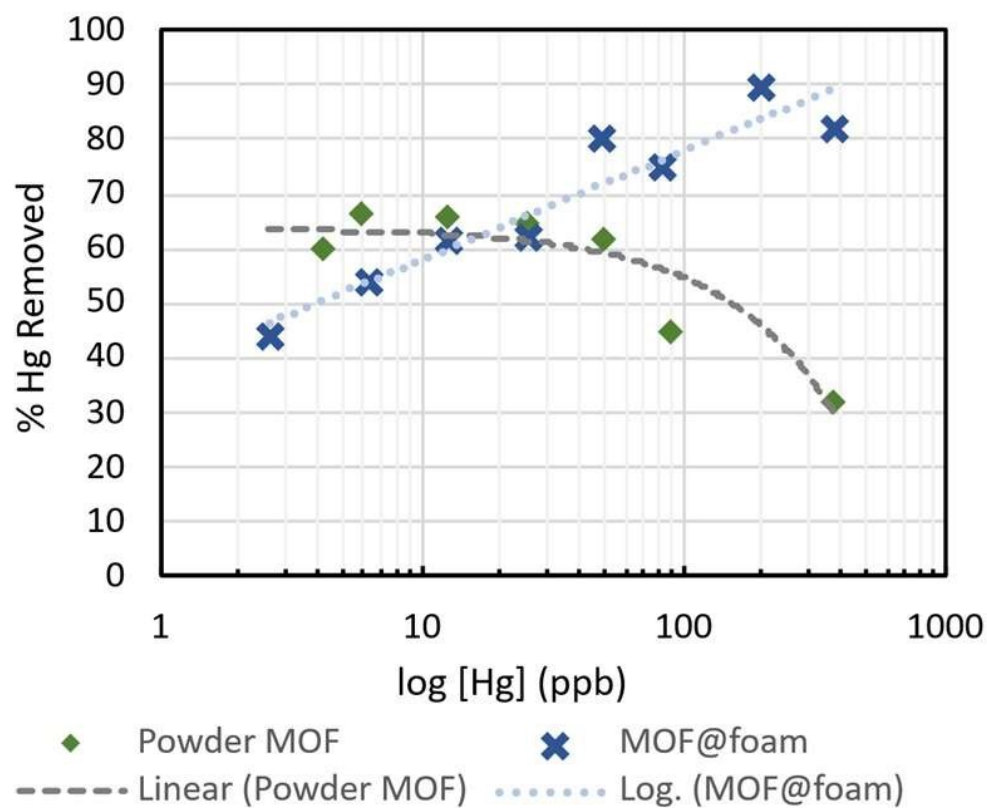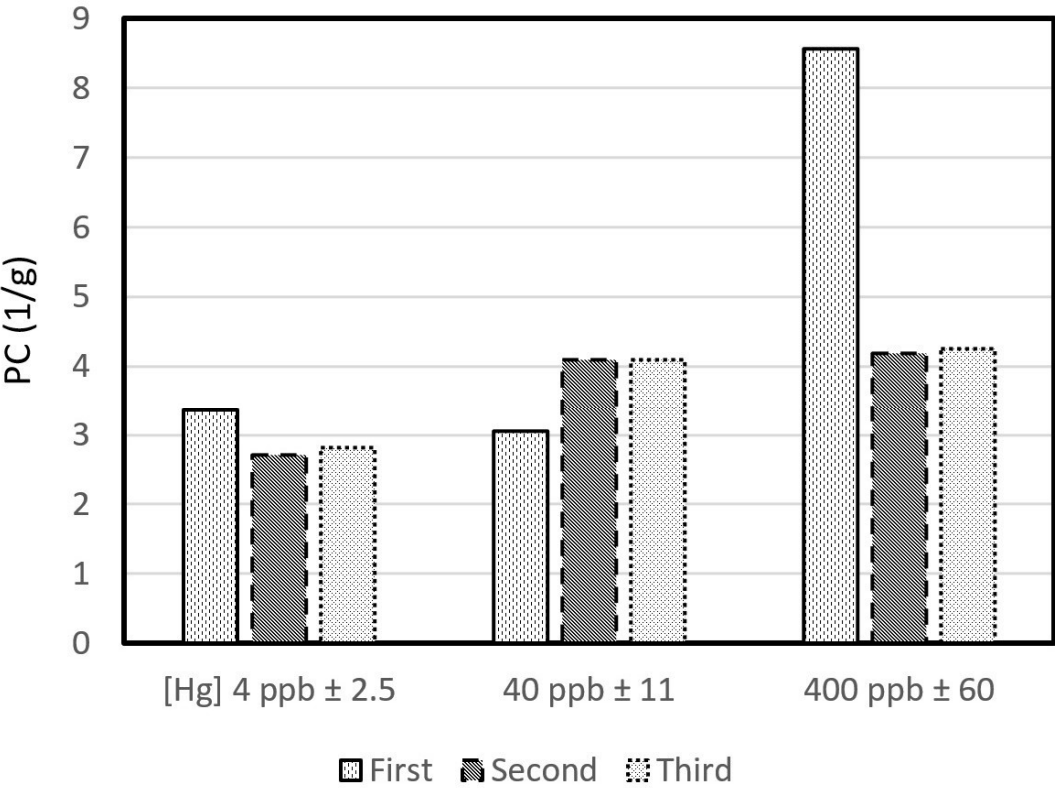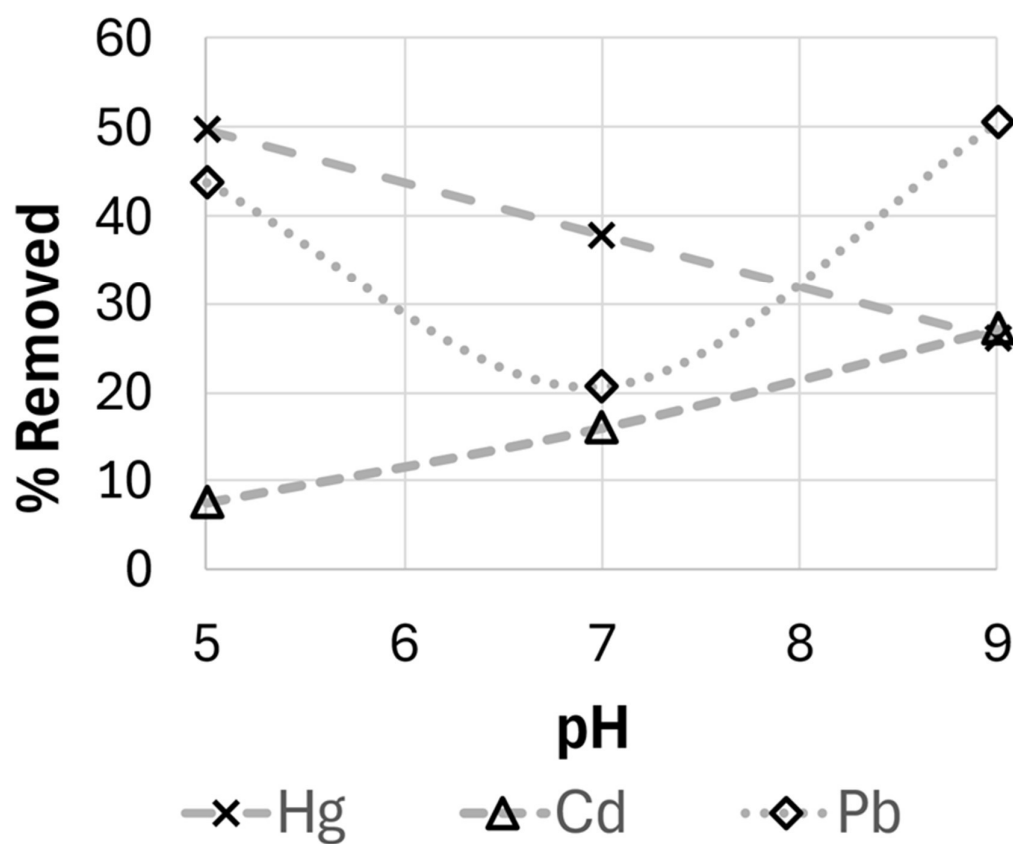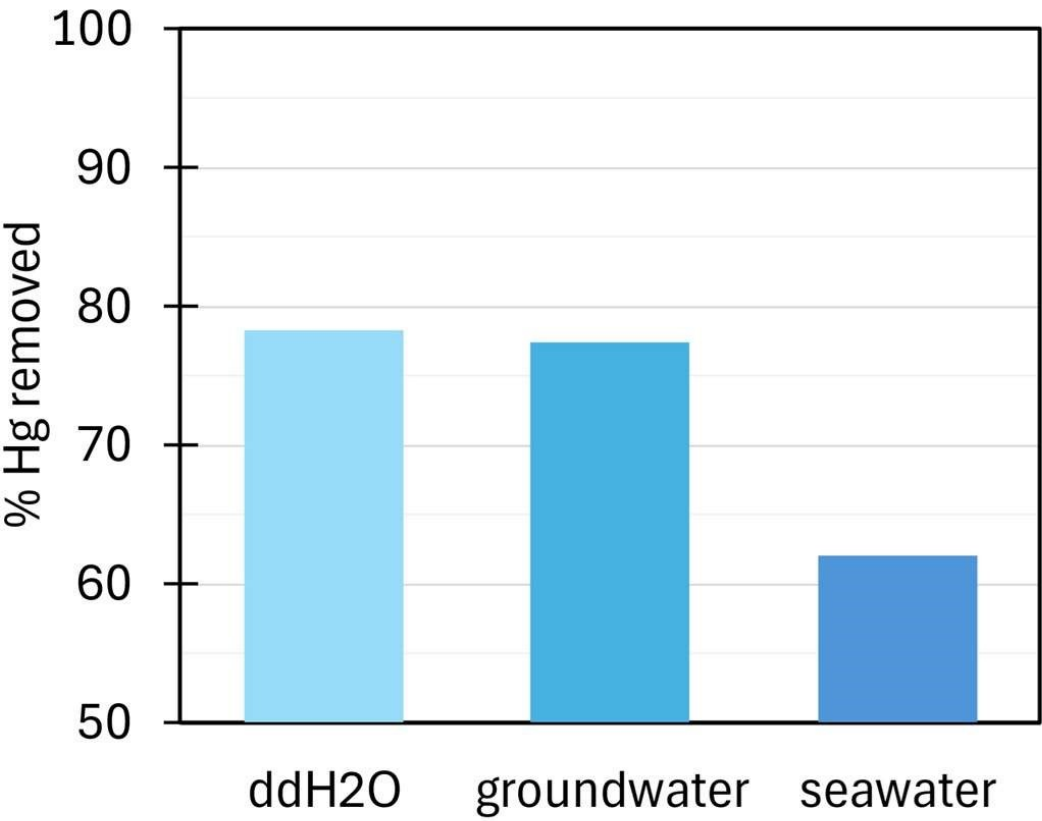
Figure 8

Figure 9

Data Availability Statement for Paper:

Novel MOF Grown on Ni foam as a Ex Situ Absorptive Medium for the Remediation of Hg

Polluted Water in Surface Water

Data relating to the above paper is available on request, including the raw .csv files provided by the ICP-MS machine, as well as other raw files produced by other characterization techniques. The process and product of the mathematical analysis conducted on said raw data is available in the body of the above paper, but – if so requested – can be provided in excel format.